Configuration-Specific Kinetic Theory Applied to the Elastic Collisions of Hard Spherical Molecules

Floyd L. Wiseman

Senior Scientist, ENSCO, Inc., 4849 North Wickham Road, Melbourne, Florida 32940

Received: August 25, 2005; In Final Form: March 24, 2006

Classical trajectory simulations can be used to glean a wealth of information on the geometric details of gas-phase molecular collision events for which the standard theoretical treatment lacks the ability to predict. For instance, the standard treatment gives no information on *configuration-specific* collision parameters. A configuration-specific parameter is defined here as the average value for a collision parameter that is exclusive to either an ensemble of front-end or an ensemble of rear-end molecular collisions. This paper presents statistical results of simulation "measurements" on several configuration-specific parameters, including the configuration-specific collision frequencies. The simulations use single-component systems of hard spherical molecules confined within a spherical boundary. To complement the simulation effort, a systematic mathematical analysis for the configuration-specific parameters is presented. This analysis uses the Maxwell−Boltzmann distribution of molecular speeds as usual, but exploits the distinction between front-end and rear-end collision space, and uses the line-of-centers speed rather than the relative speed. The configuration-specific expressions derived from this analysis are in very good agreement with the simulation measurements for every molecular collision parameter studied in this work.

Introduction

Brief Review of the Standard Analysis. The standard analysis for a single-component ideal gas at thermal equilibrium leads to the following expressions for the collision frequency of a single molecule, z_{AA}, the average relative collision speed, $\langle v_{rel}\rangle$, the average relative collision angle, $\langle \alpha_{rel}\rangle$, and the mean free path, λ:[1]

$$z_{AA} = \frac{P\sigma_{AA}\langle v_{rel}\rangle}{kT} \tag{1}$$

$$\langle v_{rel}\rangle = \sqrt{2}\langle v\rangle \tag{2}$$

$$\langle \alpha_{rel}\rangle = \frac{\pi}{2} \tag{3}$$

$$\lambda = \frac{\langle v\rangle}{z_{AA}} = \frac{kT}{\sqrt{2}P\sigma_{AA}} \tag{4}$$

in which $\langle v\rangle$ is the average thermal molecular speed, k is Boltzmann's constant (1.3807×10^{-23} J/K), and σ_{AA} is the collision cross section. The total collision frequency, Z_{AA}, depends on z_{AA} and the number of molecules, N, as follows:

$$Z_{AA} = \frac{Nz_{AA}}{2} = \frac{PN\sigma_{AA}\langle v_{rel}\rangle}{2kT} \tag{5}$$

in which the factor of $^1/_2$ is introduced to avoid counting molecular collisions twice. The expression for $\langle v\rangle$ can be derived from the following integral expression:

$$\langle v\rangle = \int_0^\infty v f(v)\, \mathrm{d}v \tag{6}$$

in which $f(v)\delta v$ is the Maxwell−Boltzmann distribution of speeds given by

$$f(v)\delta v = \frac{4}{\sqrt{\pi}}\beta^{3/2}v^2 \mathrm{e}^{-\beta v^2}\delta v \tag{7}$$

and $\beta = m/2kT$. Evaluating eq 6 yields

$$\langle v\rangle = \sqrt{\frac{8kT}{\pi m}} = \sqrt{\frac{4}{\pi\beta}} \tag{8}$$

It is useful to briefly recap the standard method for deriving eq 1, which is discussed in detail in ref 2. Initially a system of gaseous molecules is treated as completely static except for one single molecule, hereafter called the test molecule. In time t, the test molecule sweeps out an average cylindrical volume element given by $\sigma_{AA}\langle v\rangle t$. The test molecule will collide with any molecule whose center of mass is located within this volume element. To account for full molecular motion of the system, $\langle v\rangle$ is replaced with $\langle v_{rel}\rangle$. The corrected volume element, $\sigma_{AA}\langle v_{rel}\rangle t$, is then multiplied by the number of molecules per unit volume, which is P/kT for an ideal gas, to obtain the number of collisions, $P\sigma_{AA}\langle v_{rel}\rangle t/kT$, occurring in time t. This expression is then divided by t to obtain eq 1.

The Basic Concept of Configuration-Specific Analysis. A careful examination of the geometric details of molecular collisions reveals certain dynamic features that are not taken into account in the standard analysis. One feature is that all molecular collisions occur either in a front-end or in a rear-end configuration. In a front-end configuration the component line-of-centers velocity vectors are oriented "head-to-head" (schematically represented as → ←), whereas in a rear-end configuration they are oriented "head-to-tail" (→ → or ← ←). Although most physical chemistry textbook authors recognize that rear-end collisions do occur, they do not treat the system as separate ensembles of front-end and rear-end collision events. Most authors treat the system by simply using the average molecular speed, $\langle v\rangle$, in their analyses rather than the more

10.1021/jp054813r CCC: $33.50
Published on Web 04/25/2006

rigorous method using the distribution of speeds, $f(v)\delta v$. If all the molecules were actually traveling at the average speed, then only front-end collisions could occur. Hence, it stands to reason that configuration-specific analysis requires using $f(v)\delta v$. The mathematical approach for addressing configuration-specificity is a bit more detailed than the standard analysis, but has the distinct benefit of rendering configuration-specific collision parameters.

One final feature that has not been considered within the context of kinetic molecular theory is the use of the line-of-centers speed, v_{lc}, rather than the relative speed, v_{rel}, in the analysis. The chief motivation for this choice is that v_{rel} does not contain the geometric information required to derive configuration-specific parameters. Understanding the distinction between v_{rel} and v_{lc} is important, and so the next subsection briefly examines the fundamental relationship between v_{rel} and v_{lc}.

The Relationship between v_{rel} and v_{lc}. The relative speed, v_{rel}, between two molecules is[3]

$$v_{rel}(\alpha,v_1,v_2) = \sqrt{\mathbf{v_{rel}}\cdot\mathbf{v_{rel}}} = \sqrt{(\mathbf{v_1}-\mathbf{v_2})\cdot(\mathbf{v_1}-\mathbf{v_2})} = \sqrt{v_1^2 + v_2^2 - 2v_1v_2\cos\alpha} \quad (9)$$

in which $\mathbf{v_{rel}}$ is the relative velocity vector, $\mathbf{v_1}$ and $\mathbf{v_2}$ are the velocity vectors for molecules 1 and 2, respectively, and $\cos\alpha = \mathbf{v_1}\cdot\mathbf{v_2}/\mathbf{v_1}\mathbf{v_2}$. Note that v_1 and v_2 are positive scalar quantities. The general integral expression for $\langle v_{rel}\rangle$ can be generated as follows using $v_{rel}(\alpha,v_1,v_2)$, the Maxwell−Boltzmann distribution of speeds represented by $f(v_1)$ and $f(v_2)$, and the angular probability distribution function represented by $P(\alpha)\delta\alpha$:

$$\langle v_{rel}\rangle = \int_0^{\pi}\int_0^{\infty}\int_0^{\infty} v_{rel}(\alpha,v_1,v_2)f(v_1)f(v_2)P(\alpha)\,dv_1\,dv_2\,d\alpha \quad (10)$$

The angular probability distribution function, defined as the probability that v_1 and v_2 will be oriented between α and $\alpha + \delta\alpha$ relative to each other, is given as follows for the angular range, $0 \le \alpha \le \pi$:[4]

$$P(\alpha)\delta\alpha = \frac{\sin\alpha\delta\alpha}{2} \quad (11)$$

Evaluating eq 10 yields eq 2.

The line-of-centers speed, which is scalar, is defined as the negative time rate of change of the distance, r_{12}, between the centers of mass of two bodies, i.e.:

$$v_{lc} = -\frac{\delta r_{12}}{\delta t} \quad (12)$$

The line-of-centers speed, v_{lc}, and the relative velocity, v_{rel}, are related via the following dot product expression[5]

$$v_{lc} = -v_{rel}.u_{12} = (\mathbf{v_1}-\mathbf{v_2})\cdot\mathbf{u_{12}} \quad (13)$$

in which u_{12} is the unit vector along the axis joining the centers of mass. The dot products, $v_1\cdot u_{12}$ and $v_2\cdot u_{12}$, can be replaced with their scalar terms to yield

$$v_{lc}(\alpha_1,\alpha_2,v_1,v_2) = v_1\cos\alpha_1 - v_2\cos\alpha_2 \quad (14)$$

The line-of-centers speed is the scalar projection of v_{rel} onto the internuclear axis, and $v_1\cos\alpha_1$ and $v_2\cos\alpha_2$ are the scalar projections of v_1 and v_2, respectively, onto the internuclear axis. The angular variables, α_1 and α_2, not to be confused with α in the expression for $v_{rel}(\alpha,v_1,v_2)$, are hereafter called the collision angles.

Equation 14 is a general expression that is true irrespective of the shape of the molecules or whether a collision actually occurs. However, for a collision event eq 14 is sufficiently informative only if the two bodies are spherical. The details of a molecular collision involve complicated expressions of orientation vectors if either or both molecules are structured. In addition, σ_{AA} becomes orientation dependent as well. Hence, to keep the analysis simple, discussions in this paper are limited to spherical molecules.

As a side note, $v_{rel}(\alpha,v_1,v_2)$ remains constant for any pair of noninteracting molecules until a collision involving one or both molecules occurs. On the other hand, even for noninteracting molecules $v_{lc}(\alpha_1,\alpha_2,v_1,v_2)$ continuously varies because α_1 and α_2 continuously vary. The only exception is when v_1 and v_2 are collinear, in which case $v_{lc}(\alpha_1,\alpha_2,v_1,v_2) = v_{rel}(\alpha,v_1,v_2)$. Of course, the probability for a collinear orientation is vanishingly small.

Chapman and Cowling[6] have pointed out that analyzing certain collision parameters requires two internal scalar coordinates. Obviously, since $v_{rel}(\alpha,v_1,v_2)$ depends on only one scalar coordinate, there are certain parameters that cannot be analyzed using $v_{rel}(\alpha,v_1,v_2)$. Among these include configuration-specific collision parameters. The use of $v_{rel}(\alpha,v_1,v_2)$ in the analysis leads exclusively to non-configuration-specific (or overall) collision parameters, such as those given in eqs 1−4.

A collision can occur only if $v_{lc}(\alpha_1,\alpha_2,v_1,v_2) > 0$. In front-end collisions $v_{lc}(\alpha_1,\alpha_2,v_1,v_2)$ is always positive irrespective of the speeds of the colliding molecules. For this reason there are no speed restrictions in the analyses of front-end configuration-specific parameters. On the other hand, in the analyses for rear-end configuration-specific parameters a restriction must be placed upon the minimum speed of one of the molecules to ensure that $v_{lc}(\alpha_1,\alpha_2,v_1,v_2) > 0$. As will be demonstrated shortly, this distinct feature of rear-end collisions reduces the probability of rear-end collisions, making front-end collisions more probable than rear-end collisions.

Fortunately, the theoretical expressions for the various configuration-specific collision parameters derived in this paper can easily be "measured" using trajectory simulation methods. Results from simulation studies on several systems is presented in the Results and Discussion, and the data compare quite well with the theoretical predictions.

Theory

Expressions for $Z_{AA,front}$ and $Z_{AA,rear}$. Configuration specificity can be captured in the analysis using the *differential collision frequency*. The general expression for the differential collision frequency between two different types of molecules, δZ_{AB}, used by Kauzmann in his derivation of Z_{AB} is[7]

$$\delta Z_{AB} = \frac{\sigma_{AB}v_{rel}\delta N_{v_A}\delta N_{v_B}}{V} \quad (15)$$

in which σ_{AB} is the collision cross section given by $\sigma_{AB} = \pi(r_A + r_B)^2$ (r_A and r_B are the molecular radii), and δN_{v_i} is the number of i molecules (i is A or B) having speeds between v_i and $v_i + \delta v_i$. Equation 15 is not yet complete since it does not contain the angular probability distribution function. This function will be added in a moment. Using Kauzmann's line of thought, the differential collision frequency between molecules *of the same*

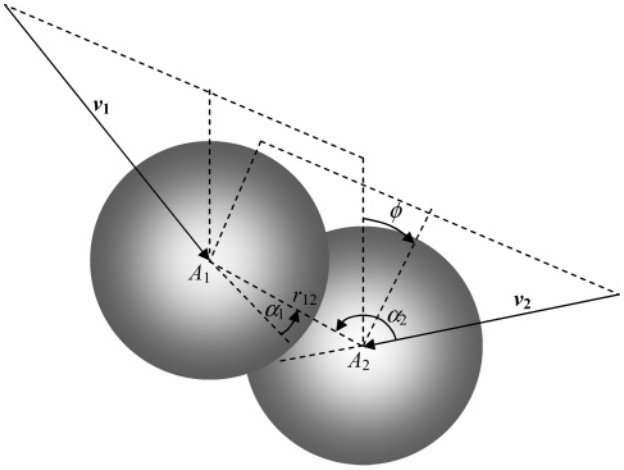

Figure 1. Representative configuration for a front-end collision between two spherical molecules. Points A_1 and A_2 define the spatial coordinates for the centers of mass for molecules 1 and 2, respectively, and r_{12} is the internuclear distance between the centers of mass when the molecules are touching. Note that molecule 1 is in the foreground. The dihedral angle, ϕ, is the angle between the planes defined by $\mathbf{v_1}$ and $\mathbf{u_{12}}$, and $\mathbf{v_2}$ and $\mathbf{u_{12}}$. The quantities, υ_1, υ_2, α_1, and α_2, are independent of ϕ and r_{12} for spherical molecules.

type can be written as

$$\delta Z_{AA} = \frac{\sigma_{AA} \upsilon_{rel} \delta N_{\upsilon_1} \delta N_{\upsilon_2}}{2V} \tag{16}$$

in which the factor of $^1/_2$ ensures that molecular collisions are counted only once. The general expression for δN_{υ_i} is given by the following modified form of eq 7:

$$\delta N_{\upsilon_i} = Nf(\upsilon_i)\delta\upsilon_i = \frac{4N}{\sqrt{\pi}}\beta^{3/2}\upsilon_i^2 e^{-\beta\upsilon^2}\delta\upsilon_i \tag{17}$$

The expression for δZ_{AA} in eq 16 is not configuration specific since it does not contain $\upsilon_{lc}(\alpha_1,\alpha_2,\upsilon_1,\upsilon_2)$. If $\upsilon_{rel}(\alpha,\upsilon_1,\upsilon_2)$ is replaced with $\upsilon_{lc}(\alpha_1,\alpha_2,\upsilon_1,\upsilon_2)$, however, the expression for δZ_{AA} becomes configuration specific. For configuration-specific collision space the angular probability distribution function defines the probability for a collision in which molecule 1 approaches at an angle between α_1 and $\alpha_1 + \delta\alpha_1$ and molecule 2 at an angle between α_2 and $\alpha_2 + \delta\alpha_2$ (see Figure 1). This angular probability distribution function is

$$P(\alpha_1,\alpha_2) = \sin\alpha_1 \sin\alpha_2 \delta\alpha_1 \delta\alpha_2 \tag{18}$$

The factor of $^1/_2$ in the expression for $P(\alpha)$ does not appear in the expression for $P(\alpha_1,\alpha_2)$ because, as will be shown momentarily, the angular functions containing α_1 and α_2 are each integrated over a range of $\pi/2$ rather than π. Putting the functions for $\upsilon_{lc}(\alpha_1,\alpha_2,\upsilon_1,\upsilon_2)$, δN_{υ_1}, δN_{υ_2}, and $P(\alpha_1,\alpha_2)$ into eq 16 and replacing N/V with P/kT yields

$$\delta Z_{AA}(\alpha_1,\alpha_2,\upsilon_1,\upsilon_2) = \frac{8NP\sigma_{AA}\beta^3}{\pi kT}\sin\alpha_1 \sin\alpha_2 \upsilon_1^2\upsilon_2^2 (\upsilon_1\cos\alpha_1 - \upsilon_2\cos\alpha_2)e^{-\beta_{\upsilon_1}^2}e^{-\beta_{\upsilon_2}^2}\delta\alpha_1\delta\alpha_2\delta\upsilon_1\delta\upsilon_2 \tag{19}$$

The regions of configuration-specific collision space are defined by the limits of the integrations. For the front-end configuration, α_1 varies between 0 and $\pi/2$, α_2 varies between $\pi/2$ and π, and the molecular speeds vary between 0 and ∞ as usual. Evaluating the integral form of eq 19 using the limits for a front-end configuration yields:[8]

$$Z_{AA,front} = \int_0^\infty\int_0^\infty\int_{\pi/2}^{\pi}\int_0^{\pi/2} dZ_{AA}(\alpha_1,\alpha_2,\upsilon_1,\upsilon_2) = \frac{PN\sigma_{AA}\langle\upsilon\rangle}{2kT} \tag{20}$$

The front-end collision frequency, $Z_{AA,front}$, is smaller than Z_{AA} by the factor $1/\sqrt{2}$.

For rear-end collisions either α_1 and α_2 both vary between 0 and $\pi/2$ (i.e., $1 \rightarrow 2 \rightarrow$), or between $\pi/2$ and π (i.e., $\leftarrow 1 \leftarrow 2$). To ensure that $\upsilon_{lc}(\alpha_1,\alpha_2,\upsilon_1,\upsilon_2)$ is positive everywhere then for the case in which $0 \le \alpha_1,\alpha_2 \le \pi/2$, υ_1 must vary between $(\upsilon_2 \cos\alpha_2)/(\cos\alpha_1)$ and ∞, and for the case in which $\pi/2 \le \alpha_1,\alpha_2 \le \pi$, υ_2 must vary between $(\upsilon_1 \cos\alpha_1)/(\cos\alpha_2)$ and ∞. The expression for the rear-end collision frequency therefore contains two separate, but numerically identical terms that upon evaluation yield

$$Z_{AA,rear} = \int_0^\infty\int_{\gamma_1}^\infty\int_0^{\pi/2}\int_0^{\pi/2} dZ_{AA}(\alpha_1,\alpha_2,\upsilon_1,\upsilon_2) + \int_{\gamma_2}^\infty\int_0^\infty\int_{\pi/2}^{\pi}\int_{\pi/2}^{\pi} dZ_{AA}(\alpha_1,\alpha_2,\upsilon_1,\upsilon_2)$$

$$Z_{AA,rear} = \frac{(\sqrt{2}-1)PN\sigma_{AA}\langle\upsilon\rangle}{2kT} \tag{21}$$

in which $\gamma_1 = (\upsilon_2\cos\alpha_2)/(\cos\alpha_1)$ and $\gamma_2 = (\upsilon_1\cos\alpha_1)/(\cos\alpha_2)$. The rear-end collision frequency, $Z_{AA,rear}$, is smaller than Z_{AA} by the factor $1 - 1/\sqrt{2}$.

The overall collision frequency is simply the sum of $Z_{AA,front}$ and $Z_{AA,rear}$, i.e.:

$$Z_{AA} = Z_{AA,front} + Z_{AA,rear} = \frac{PN\sigma_{AA}\langle\upsilon\rangle}{\sqrt{2}kT} \tag{22}$$

As expected, the configuration-specific analysis yields the same expression for Z_{AA} as the standard analysis.

The fraction of front-end collisions, η_{front}, is

$$\eta_{front} = \frac{Z_{AA,front}}{Z_{AA}} = \frac{1}{\sqrt{2}} \tag{23}$$

Note that η_{front} is also the probability for a front-end collision. Equation 23 predicts that about 70.7% of all collisions for hard, noninteracting spherical molecules at thermal equilibrium are front-end collisions. This prediction agrees very well with simulation data.

Expressions for $\langle\upsilon_{lc,front}\rangle$ and $\langle\upsilon_{lc,rear}\rangle$. The fundamental expression for the average configuration-specific line-of-centers speed, $\langle\upsilon_{lc,k}\rangle$, is

$$\langle\upsilon_{lc,k}\rangle = \frac{1}{Z_{AA,k}}\int_k \upsilon_{lc}(\alpha_1,\alpha_2,\upsilon_1,\upsilon_2)\, dZ_{AA}(\alpha_1,\alpha_2,\upsilon_1,\upsilon_2) \tag{24}$$

in which the integral is over the configuration-specific region of collision space represented by k. The configuration-specific differential term, $\delta Z_{AA}(\alpha_1,\alpha_2,\upsilon_1,\upsilon_2)/Z_{AA,k}$, is the complementary term that replaces $f(\upsilon)\delta\upsilon$ for analyzing average values for configuration-specific collision parameters. As such, it can be shown that

$$\frac{1}{Z_{AA,k}}\int_k dZ_{AA}(\alpha_1,\alpha_2,\upsilon_1,\upsilon_2) = 1 \tag{25}$$

From eq 24, $\langle\upsilon_{lc,front}\rangle$ and $\langle\upsilon_{lc,rear}\rangle$ can be shown to be,

respectively:

$$\langle v_{lc,front}\rangle = \frac{1}{2}\left(1+\frac{\pi}{2}\right)\langle v\rangle \approx 1.2854\langle v\rangle \quad (26)$$

$$\langle v_{lc,rear}\rangle = \frac{(\sqrt{2}+1)}{2}\left(\frac{\pi}{2}-1\right)\langle v\rangle \approx 0.68901\langle v\rangle \quad (27)$$

The average configuration-specific line-of-centers speeds, $\langle v_{lc,front}\rangle$ and $\langle v_{lc,rear}\rangle$, are smaller than $\langle v_{rel}\rangle$ by the factors, $(2+\pi)/(4\sqrt{2})$ ($\sim$0.90891) and $((\sqrt{2}+1)(\pi-2))/(4\sqrt{2})$ ($\sim$0.48721), respectively. Moreover, $\langle v_{lc,front}\rangle$ is nearly 87% larger than $\langle v_{lc,rear}\rangle$.

Configuration-Specific Collision Probabilities and Mean Free Paths. Because there are two types of collisions in a single-component system, there are four possible patterns of $k-k'$ collision sequences, which in turn define four distinct types of *configuration-specific* mean free paths. It should be noted, however, that a $k-k'$ collision *sequence* may not occur in *succession*. The difference between sequential and successive collisions as defined here is there are no intermediate collisions between successive collisions, whereas there may be intermediate collisions between a specified collision sequence. For example, one or more front-end collisions may occur between two sequential rear-end collisions. Since the probability for any single type of collision is less than 1, the configuration-specific mean free paths are all larger than the overall mean free path given by eq 4.

Whereas configuration-specific mean free paths are defined in terms of specified sequential collisions, the overall mean free path is defined in terms of successive collisions. Noting that the probabilities for front- and rear-end collisions are $1/\sqrt{2}$ and $1-1/\sqrt{2}$, respectively (see eq 23), the expressions for the probabilities for *successive* $k-k'$ collisions, $p_{k-k'}$, are

$$p_{front-front} = \left(\frac{1}{\sqrt{2}}\right)^2 = \frac{1}{2} \quad (28)$$

$$p_{front-rear} = p_{rear-front} = \left(\frac{1}{\sqrt{2}}\right)\left(1-\frac{1}{\sqrt{2}}\right) \approx 0.20711 \quad (29)$$

$$p_{rear-rear} = \left(1-\frac{1}{\sqrt{2}}\right)^2 \approx 0.085785 \quad (30)$$

It can be easily shown that $\sum_k \sum_{k'} p_{k-k'} = 1$.

Expressions for $\langle v_{front}\rangle$, $\langle v_{rear,fast}\rangle$, and $\langle v_{rear,slow}\rangle$. The average speed for molecules involved in a configuration-specific collision of type k is:

$$\langle v_k\rangle = \frac{1}{Z_{AA,k}}\int_k v_i \, dZ_{AA}(\alpha_1,\alpha_2,v_1,v_2) \quad (31)$$

Equation 31 differs from the expression for $\langle v_{lc,k}\rangle$ in eq 24 in that eq 31 refers to the average speed of the individual molecules that undergo collisions, whereas eq 24 refers to the average line-of-centers speed of two colliding molecules. The expression for $\langle v_{front}\rangle$ given below can be derived using $i = 1$ or 2 in eq 31.

$$\langle v_{front}\rangle = \frac{1}{16}(8+3\pi)\langle v\rangle \approx 1.0891\langle v\rangle \quad (32)$$

The reason that $\langle v_{front}\rangle$ is slightly larger than $\langle v\rangle$ is explained as follows. The probability of a collision in any given time increment increases with the speed of a molecule. This effect is offset by the fact that the fraction of molecules having speeds higher than the most probable speed decreases as the speed increases, in accordance with the Maxwell−Boltzmann distribution. Equation 31 accounts for these two effects, and the net result is $\langle v_{front}\rangle$ is larger than $\langle v\rangle$.

On average the speeds of molecules that engage a front-end collision are the same. However, this is not the case for rear-end collisions, in which the average speed for the molecules that are coming from behind in the collisions is somewhat larger than that of the molecules that are in front. The analysis for rear-end collisions therefore leads to two average speeds which can be shown to be

$$\langle v_{rear,fast}\rangle = \frac{(\pi-1)(\sqrt{2}+1)\langle v\rangle}{4} \approx 1.2926\langle v\rangle \quad (33)$$

$$\langle v_{rear,slow}\rangle = \frac{(6-\pi)(\sqrt{2}+1)\langle v\rangle}{8} \approx 0.86260\langle v\rangle \quad (34)$$

in which "*fast*" refers to the faster molecule that is behind, and "*slow*" to the slower molecule that is in front.

Expressions for $\langle \alpha_{lc,front}\rangle$, $\langle \alpha_{lc,rear,fast}\rangle$, and $\langle \alpha_{lc,rear,slow}\rangle$. The general expression for the average line-of-centers collision angle, $\langle \alpha_{lc,k}\rangle$, is

$$\langle \alpha_{lc,k}\rangle = \frac{1}{Z_{AA,k}}\int_k \alpha_i \, dZ_{AA}(\alpha_1,\alpha_2,v_1,v_2) \quad (35)$$

Expressions for $\langle \alpha_{lc,front}\rangle$, $\langle \alpha_{lc,rear,fast}\rangle$, and $\langle \alpha_{lc,rear,slow}\rangle$ derived from eq 35 are, respectively:

$$\langle \alpha_{lc,front}\rangle = \frac{1}{2}\left(1+\frac{\pi}{4}\right) \approx 51.148^\circ \quad (36)$$

$$\langle \alpha_{lc,rear,fast}\rangle = \frac{1}{2}(\sqrt{2}-1)\left(\frac{\pi}{2}-1\right) \approx 39.478^\circ \quad (37)$$

$$\langle \alpha_{lc,rear,slow}\rangle = \frac{\sqrt{2}+1}{2} \approx 69.162^\circ \quad (38)$$

The expression for $\langle \alpha_{lc,front}\rangle$ can be derived using $i = 1$ or 2. The expression for $\langle \alpha_{lc,rear,fast}\rangle$ can be derived using $i = 1$ and integrating α_1 and α_2 between 0 and $\pi/2$, v_1 between 0 and ∞, and v_2 between γ_1 and ∞; or it can be derived using $i = 2$ and integrating α_1 and α_2 between $\pi/2$ and π, v_1 between γ_2 and ∞, and v_2 between 0 and ∞. The expression for $\langle \alpha_{lc,rear,slow}\rangle$ can be derived using $i = 2$ and integrating α_1 and α_2 between 0 and $\pi/2$, v_1 between 0 and ∞, and v_2 between γ_1 and ∞; or it can be derived using $i = 1$ and integrating α_1 and α_2 between $\pi/2$ and π, v_1 between γ_2 and ∞, and v_2 between 0 and ∞.

Simulation Methodology. The trajectory simulations in this work use the classical motion equations that conserve momentum and energy for elastic collisions. The systems consist of smooth spherical molecules confined inside a spherical container whose center is at the origin of the coordinate system. The radius of the container, r_{cont}, is related to T, P, and N, as illustrated in the following analysis. The volume of the container, V_{cont}, is

$$V_{cont} = \frac{4\pi r_{cont}^{\ 3}}{3} \quad (39)$$

Equating V_{cont} to the volume of an ideal gas, $V = NkT/P$, and rearranging yields the following expression for r_{cont}:

$$r_{cont} = \left(\frac{3NkT}{4\pi P}\right)^{1/3} \quad (40)$$

The molecules are initially placed inside a cubical box that is inscribed within the spherical container. This method is chosen

because the algorithm for placing molecules in an ordered array is much simpler for a cubical geometry than a spherical geometry. The cross diagonal of the inscribed box is equal to the diameter of the sphere, and so the length of each edge of the box, s_{box}, is $2r_{cont}/\sqrt{3}$. The box is subdivided into small unit cells, each of which contains one molecule at the beginning of the simulation run. The unit cell length, s_{cell}, is

$$s_{cell} = \frac{s_{box}}{N^{1/3}} = \frac{2}{\sqrt{3}}\left(\frac{3kT}{4\pi P}\right)^{1/3} \tag{41}$$

The molecules are randomly offset between ~0 and ~r_A in each coordinate from the centers of the cells to ensure positional and directional randomization once the molecules are in motion and begin colliding.

There are two sources of systematic error that arise because of nonideality in these systems. One source arises from the fact that the free volume is slightly reduced due to the finite volume of the molecules. This error can be corrected by using the effective system pressure, P_{eff}, in the expressions for the collision frequencies (eqs 20, 21, and 22) and the mean free path (eq 4). The expression for P_{eff} is given as

$$P_{eff} = P\left(\frac{{r_{cont}}^3}{{r_{cont}}^3 - N{r_A}^3}\right) \tag{42}$$

The second source of error arises from the fact that r_A is not negligibly small relative to r_{cont}. The correction for this error will be discussed in a moment.

Once in motion, the molecules are confined to the spherical container via reverse reflection (reversing the sign of the component velocity vectors of a molecule when it hits the wall). Because molecules collide with the wall at random orientations, they are reflected at random orientations. In principle, therefore, randomness should not be compromised as a result of reflection. Simulation studies in which the radial concentration gradients were closely monitored show that there are no permanent gradients anywhere in the system once it has equilibrated (there are, however, local fluctuations.) This overall uniformity in concentration suggests that there are no directional biases or systematic deviations from the Maxwell−Boltzmann distribution resulting from reflection at the wall.

Both types of collision events, molecule-with-molecule (m−m) and molecule-with-wall (m−w), are elastic. Energy and momentum are conserved in the m−m collisions, and energy and the magnitudes of the momentum vectors are conserved in the m−w collisions.

The component velocity vectors for each molecule are chosen so that each molecule has an initial speed equal to the root-mean-square speed. This ensures the system has the correct kinetic energy, which is $3NkT/2$. The magnitudes of the vectors are all equivalent, but the signs are randomized to ensure the net momentum in each coordinate is close to zero. The total system energy and the sum of momenta in each coordinate are monitored to ensure numerical integrity and motion randomness.

The user-input standard time step, Δt_{stand}, is on the order of 10^{-14} s. The standard average positional advancement per time step, given by $\langle \Delta r_{stand} \rangle = \langle \upsilon \rangle \Delta t_{stand}$, is on the order of 0.01 nm. Because Δt_{stand} is finite, some degree of overlap occurs with each detected collision event. An m−m overlap between molecules i and j occurs if the following condition is encountered:

$$\sqrt{(x_j - x_i)^2 + (y_j - y_i)^2 + (z_j - z_i)^2} < 2r_A \tag{43}$$

Analogously, an m−w overlap for molecule i occurs if the following condition is encountered

$$\sqrt{x_i^2 + y_i^2 + z_i^2} > r_{cont} - \tau r_A \tag{44}$$

in which τ is the adjustment factor that compensates for nonideality arising from r_A being nonnegligible relative to r_{cont}. For a physically realistic m−w collision, represented by $\tau = 1$, the molecules are reflected at the point they hit the wall. However, the simulation values for Z_{AA} are as much as ~3% high and those for λ as much as ~3% low when $\tau = 1$. The agreement can be brought within a fraction of a percent using the adjustment technique for τ that will be discussed in a moment.

The algorithm described as follows calculates the time of overlap, which is defined as the amount of time during which the condition described by either eq 43 or 44 holds true. All possible collision events are tested for overlap for each molecule at each time step. For each detected collision event, the time of overlap is determined by the degree of motion reversal required to ensure one of the following two conditions is met, whichever applies:

$$\sqrt{(x_j - x_i)^2 + (y_j - y_i)^2 + (z_j - z_i)^2} = 2r_A \quad \text{(m-m collision)} \tag{45}$$

$$\sqrt{x_i^2 + y_i^2 + z_i^2} = r_{cont} - \tau r_A \quad \text{(m-w collision)} \tag{46}$$

The entire system of molecules is then motion reversed according to the collision event having the *maximum overlap time*, Δt_{max}. The actual time step, Δt_{act}, then becomes

$$\Delta t_{act} = \Delta t_{stand} - \Delta t_{max} \tag{47}$$

After the time step is adjusted via eq 47, the only molecule(s) that is(are) still in contact is(are) the one(s) with the maximum overlap time. The appropriate recoil equations are applied to this (these) molecule(s) before the next time step.

It is duly noted here that a small fraction of glancing m−m collisions can be missed using this approach. This fraction should become smaller as the value of Δt_{stand} is reduced. Simulation studies using a range of values for Δt_{stand} indicate that the number of collisions that might be missed is negligibly small for the range used in this work.

The adjustment for τ is described as follows. The ratio of the simulation collision frequency, $Z_{AA,sim}$, to the theoretical collision frequency, $Z_{AA,theory}$, is a function of τ, i.e.

$$\frac{Z_{AA,sim}}{Z_{AA,theory}} = f(\tau) \tag{48}$$

Studies show that $f(0) < 1$ and $f(1) > 1$. Hence, there is a value of τ, hereafter called τ_{ideal}, in which $0 < \tau_{ideal} < 1$ and $f(\tau_{ideal}) = 1$ within random error. Noting that the collision frequency is inversely proportional to the volume, which is $(4\pi(r_{cont} - \tau r_A)^3)/(3)$, the ratio of $f(1)$ to $f(\tau_{ideal})$ can be shown to be

$$\frac{f(1)}{f(\tau_{ideal})} = f(1) = \left(\frac{r_{cont} - \tau_{ideal} r_A}{r_{cont} - r_A}\right)^3 \tag{49}$$

TABLE 1: Results of Classical Trajectory Simulations and Theoretical Predictions for a Series of Systems Having Various Values for r_{cont} and N[a]

r_{cont}/nm		results		errors	
N		theoretical	simulation[b]	random	systematic
10.68	Z_{AA}/s^{-1}	5.452×10^{11}	$5.614(\pm0.029) \times 10^{11}$	0.52	3.0
125	λ/nm	32.69	31.74($\pm$0.16)	0.50	−2.9
14.96	Z_{AA}/s^{-1}	1.4961×10^{12}	$1.5436(\pm0.0072) \times 10^{12}$	0.47	3.2
343	λ/nm	32.69	31.69($\pm$0.15)	0.47	−3.1
21.37	Z_{AA}/s^{-1}	4.362×10^{12}	$4.448(\pm0.012) \times 10^{12}$	0.27	2.0
1000	λ/nm	32.693	32.056($\pm$0.084)	0.26	−1.9
29.92	Z_{AA}/s^{-1}	1.1968×10^{13}	$1.2149(\pm0.0018) \times 10^{13}$	0.15	1.5
2744	λ/nm	32.693	32.198($\pm$0.050)	0.16	−1.5
40.60	Z_{AA}/s^{-1}	2.9917×10^{13}	$3.0264(\pm0.0035) \times 10^{13}$	0.12	1.2
6859	λ/nm	32.693	32.299($\pm$0.039)	0.12	−1.2

[a] All of the systems have the following specifications: $T = 300$ K, $P = 1.00$ atm, $M = 78.1$ g·mol^{-1} (C_6H_6), $r_A = 0.265$ nm, $\langle \Delta r_{stand} \rangle \approx 6.27 \times 10^{-3}$ nm, $\langle v \rangle \approx 285$ m·s^{-1}, and $\tau = 1$ (fixed). [b] The 95% confidence levels are given in parentheses.

Rearranging eq 49 yields the following expression for τ_{ideal}:

$$\tau_{ideal} = f^{1/3}(1) - \frac{r_{cont}[f^{1/3}(1) - 1]}{r_A} \tag{50}$$

The simulation runs always begin with $\tau = 1$. When the system becomes well equilibrated, the value for $f(1)$ is used to calculate τ_{ideal} via eq 50. When $\tau = 1$ is replaced with $\tau = \tau_{ideal}$ in eqs 44 and 46, the values for $Z_{AA,sim}$ and λ_{sim} readjust to their new values after about $5N$ collisions. The errors for the adjusted values for $Z_{AA,sim}$ and λ_{sim} were within the random errors for every system studied in this work. However, none of the configuration-specific parameters that were monitored were noticeably affected by the value of τ for any of the systems studied.

The simulation program begins monitoring the various collision parameters after a user-specified number of m−m collisions. The total number of m−m collisions in the runs ranged from $\sim 7 \times 10^5$ for the smaller systems to $\sim 4 \times 10^6$ for the larger systems.

Each molecule has a distance tracker that uses the following expression to track the distance, d_i, traveled between successive collisions:

$$d_i = v_i \sum_{j=1}^{n_{sc}} \Delta t_{act,j} \tag{51}$$

in which n_{sc} is the number of time steps between successive collisions. The value for v_i is constant between successive collisions, whereas $\Delta t_{act,j}$ may or may not be the same for each new time step. The values for d_i are not affected by m−w collisions since molecular speeds are unchanged by reflective collisions. Once the second collision in the succession occurs, the current value of d_i is used to update the average value for λ, and d_i is then reset to 0. A separate algorithm tracks $p_{k-k'}$ for each pair of successive collisions.

After about $20N$ m−m collisions the molecules become evenly distributed throughout the spherical container, the distribution of speeds very closely follows the Maxwell−Boltzmann distribution (eq 7), and the average molecular speed for the system converges to $\langle v \rangle$ within a small fraction of a percent ($\langle v \rangle$ is slightly smaller than the root-mean square speed used to initialize the speeds of the molecules.) After $\tau = 1$ is replaced with $\tau = \tau_{ideal}$, the system executes a user-specified number of time steps before beginning the statistical analysis. Between 20 and 40 sets of simulation data points were used in the statistical analysis for each run conducted in this work.

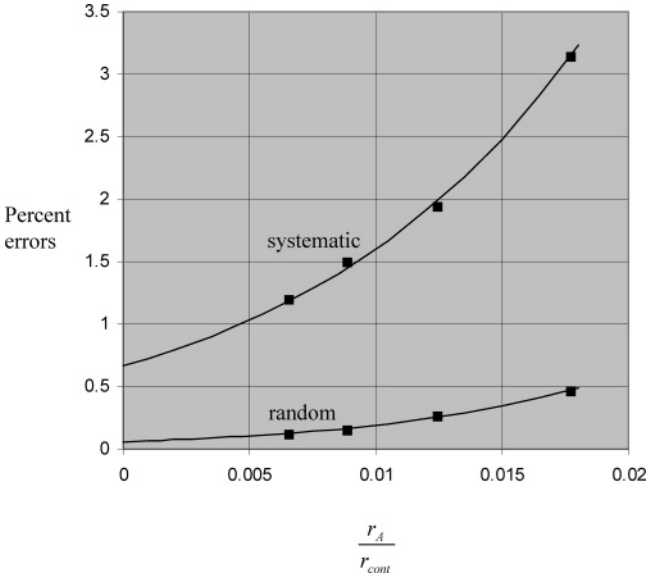

Figure 2. Graphs of $(|Error_\lambda| + Error_{Z_{AA}})/2$ vs r_A/r_{cont} for the random and systematic errors in Table 1 (excluding the first data set.) The two sets of data points were each fitted to the empirical function, $(|Error_\lambda| + Error_{Z_{AA}})/2 = a \exp(br_A/r_{cont})$. The best-fit values for the random and systematic errors are, respectively, as follows: $a = 0.0569/0.665$, and $b = 120/87.8$.

Results and Discussion

Table 1 shows simulation data and theoretical predictions for systems in which τ is fixed at 1, $r_A = 0.265$ nm, and the ratio, r_A/r_{cont}, ranges from 0.00653 to 0.0248. The purpose for conducting these runs was to assess the trend in the random and systematic errors for λ and Z_{AA} as r_A/r_{cont} and $1/N$ become smaller. The random errors are the percent errors determined from the 95% confidence levels, and the systematic errors are the percent errors determined from the differences between the theoretical and simulation values. Unfortunately, the size of the systems that can be feasibly studied is limited by computer runtime, so that only a limited range for r_A/r_{cont} is practical. Fortunately, the range for r_A/r_{cont} in this work is large enough to show that, after a threshold system size is reached, both the random and systematic errors decrease as r_A/r_{cont} and $1/N$ decrease. Figure 2 shows graphs for $(|Error_\lambda| + Error_{Z_{AA}})/2$ vs r_A/r_{cont} for the random and systematic errors. An empirical function was fitted to the two data sets. From this function the values for the random and systematic errors extrapolated to $r_A/r_{cont} = 0$ are $\sim$0.06% and $\sim$0.7%, respectively. The value for the extrapolated systematic error may be high because the systematic error for the largest system shows a distinct

TABLE 2: Results of Classical Trajectory Simulations and Theoretical Predictions for Several Collision Parameters for a System Having the Following Specifications: $T = 300$ K, $P = 1.00$ atm, $M = 28.0$ g·mol^{-1} (N_2), $r_A = 0.185$ nm, $N = 729$, $\langle \Delta r_{stand} \rangle \approx 5.23 \times 10^{-3}$ nm, $\langle v \rangle \approx 476$ m·s^{-1}, $r_{cont} \approx 19.2$ nm, and $\tau_{ideal} \approx 0.470$

parameter[a]	theoretical value	simulation value
Z_{AA}/s^{-1}	2.585×10^{12}	$2.583(\pm 0.008) \times 10^{12}$
η_f	0.7071	0.7078(±0.0014)
$\langle v_{lc,f} \rangle$/m·s^{-1}	612.2	612.2(±0.9)
$\langle v_{lc,r} \rangle$/m·s^{-1}	328.2	328.0(±1.0)
λ/nm	67.17	67.27(±0.22)
p_{f-f}	0.5000	0.5009(±0.0026)
p_{r-r}	0.085 79	$0.08610(\pm 8.1 \times 10^{-4})$
p_{f-r}	0.2071	0.2057(±0.0069)
p_{r-f}	0.2071	0.2057(±0.0069)
$\langle v_f \rangle$/m·s^{-1}	518.7	518.7(±0.5)
$\langle v_{r,f} \rangle$/m·s^{-1}	615.7	615.5(±1.2)
$\langle v_{r,s} \rangle$/m·s^{-1}	410.8	411.3(±1.0)
$\langle \alpha_{lc,f} \rangle$/deg	51.15	51.15(±0.01)
$\langle \alpha_{lc,r,f} \rangle$/deg	39.48	39.45(±0.01)
$\langle \alpha_{lc,r,s} \rangle$/deg	69.16	69.18(±0.01)

[a] The subscripts are abbreviated here as follows: f = *front*; r = *rear*; r,f = *rear,fast*; r,s = *rear,slow*.

TABLE 3: System Specifications: $T = 300$ K, $P = 1.00$ atm, $M = 28.0$ g·mol^{-1} (N_2), $r_A = 0.185$ nm, $N = 2{,}197$, $\langle \Delta r_{stand} \rangle \approx 5.23 \times 10^{-3}$ nm, $\langle v \rangle \approx 476$ m·s^{-1}, $r_{cont} \approx 27.8$ nm, and $\tau_{ideal} \approx 0.582$

parameter	theoretical value	simulation value
Z_{AA}/s^{-1}	7.790×10^{12}	$7.808(\pm 0.020) \times 10^{12}$
η_f	0.7071	0.7076(±0.0010)
$\langle v_{lc,f} \rangle$/m·s^{-1}	612.2	612.1(±0.7)
$\langle v_{lc,r} \rangle$/m·s^{-1}	328.2	328.2(±0.7)
λ/nm	67.17	67.00(±0.17)
p_{f-f}	0.5000	0.5028(±0.0015)
p_{r-r}	0.085 79	$0.08652(\pm 6.1 \times 10^{-4})$
p_{f-r}	0.2071	$0.2066(\pm 8 \times 10^{-4})$
p_{r-f}	0.2071	$0.2066(\pm 8 \times 10^{-4})$
$\langle v_f \rangle$/m·s^{-1}	518.7	518.6(±0.4)
$\langle v_{r,f} \rangle$/m·s^{-1}	615.7	615.6(±0.7)
$\langle v_{r,s} \rangle$/m·s^{-1}	410.9	410.3(±0.7)
$\langle \alpha_{lc,f} \rangle$/deg	51.15	51.14(±0.01)
$\langle \alpha_{lc,r,f} \rangle$/deg	39.48	39.53(±0.01)
$\langle \alpha_{lc,r,s} \rangle$/deg	69.16	69.21(±0.01)

downward curvature. Hence, it is quite possible that the extrapolated values for the random and systematic errors converge more closely with each other than implied by the extrapolation method used here. In any case, the trend certainly shows that the system is very close to ideal in the limit that r_A/r_{cont} approaches zero. Adjusting τ compensates for the nonideality of the system due to its finite size. As such, τ_{ideal} approaches ~1 as r_A/r_{cont} approaches zero.

Tables 2−6 show simulation measurements and theoretical predictions for several systems in which the following collision parameters were monitored: Z_{AA} (eq 22), η_{front} (eq 23), $\langle v_{lc,front} \rangle$ (eq 26), $\langle v_{lc,rear} \rangle$ (eq 27), $p_{front-front}$ (eq 28), $p_{front-rear}$ and $p_{rear-front}$ (eq 29), $p_{rear-rear}$ (eq 30), λ (eq 4), $\langle v_{front} \rangle$ (eq 32), $\langle v_{rear,fast} \rangle$ (eq 33), $\langle v_{rear,slow} \rangle$ (eq 34), $\langle \alpha_{lc,front} \rangle$ (eq 36), $\langle \alpha_{lc,rear,fast} \rangle$ (eq 37), and $\langle \alpha_{lc,rear,slow} \rangle$ (eq 38). About 75% of the simulation measurements are in exact agreement with the theoretical predictions within the 95% confidence levels.

The ratio, λ/r_{cont}, was allowed to vary over a large enough range (from ~0.63 in Table 6 to ~6.5 in Table 4) to determine whether systematic errors occur for systems in which $\lambda > r_{cont}$. The results clearly show that the behavior of the systems is not discernibly altered if $\lambda > r_{cont}$.

TABLE 4: System Specifications: $T = 300$ K, $P = 1.00$ atm, $M = 4.00$ g·mol^{-1} (He), $r_A = 0.129$ nm, $N = 1{,}000$, $\langle \Delta r_{stand} \rangle \approx 5.32 \times 10^{-3}$ nm, $\langle v \rangle \approx 1260$ m·s^{-1}, $r_{cont} \approx 21.4$ nm, and $\tau_{ideal} \approx 0.490$

parameter	theoretical value	simulation value
Z_{AA}/s^{-1}	4.559×10^{12}	$4.542(\pm 0.019) \times 10^{12}$
η_f	0.7071	0.7071(±0.0013)
$\langle v_{lc,f} \rangle$/m·s^{-1}	1620	1621(±3)
$\langle v_{lc,r} \rangle$/m·s^{-1}	868.3	869.8(±2.8)
λ/nm	138.2	138.7(±0.5)
p_{f-f}	0.5000	0.4988(±0.0025)
p_{r-r}	0.085 79	$0.08574(\pm 9.0 \times 10^{-4})$
p_{f-r}	0.2071	0.2060(±0.0011)
p_{r-f}	0.2071	0.2060(±0.0011)
$\langle v_f \rangle$/m·s^{-1}	1372	1372(±2)
$\langle v_{r,f} \rangle$/m·s^{-1}	1629	1632(±3)
$\langle v_{r,s} \rangle$/m·s^{-1}	1087	1085(±3)
$\langle \alpha_{lc,f} \rangle$/deg	51.15	51.12(±0.01)
$\langle \alpha_{lc,r,f} \rangle$/deg	39.48	39.51(±0.02)
$\langle \alpha_{lc,r,s} \rangle$/deg	69.16	69.15(±0.01)

TABLE 5: System Specifications: $T = 300$ K, $P = 1.00$ atm, $M = 78.1$ g·mol^{-1} (C_6H_6), $r_A = 0.265$ nm, $N = 1{,}728$, $\langle \Delta r_{stand} \rangle \approx 0.0106$ nm, $\langle \mathbf{v} \rangle \approx 285$ m·s^{-1}, $r_{cont} \approx 25.6$ nm, and $\tau_{ideal} \approx 0.421$

parameter	theoretical value	simulation value
Z_{AA}/s^{-1}	7.537×10^{12}	$7.548(\pm 0.014) \times 10^{12}$
η_f	0.7071	0.7075(±0.0007)
$\langle v_{lc,f} \rangle$/m·s^{-1}	366.6	366.6(±0.3)
$\langle v_{lc,r} \rangle$/m·s^{-1}	196.5	196.7(±0.3)
λ/nm	32.69	32.64(±0.06)
p_{f-f}	0.5000	0.5018 ± 0.0012)
p_{r-r}	0.085 79	$0.08639(\pm 4.8 \times 10^{-4})$
p_{f-r}	0.2071	$0.2066(\pm 4 \times 10^{-4})$
p_{r-f}	0.2071	$0.2066(\pm 4 \times 10^{-4})$
$\langle v_f \rangle$/m·s^{-1}	310.6	310.6(±0.2)
$\langle v_{r,f} \rangle$/m·s^{-1}	368.6	368.6(±0.3)
$\langle v_{r,s} \rangle$/m·s^{-1}	246.0	246.1(±0.4)
$\langle \alpha_{lc,f} \rangle$/deg	51.15	51.15(±0.01)
$\langle \alpha_{lc,r,f} \rangle$/deg	39.48	39.47(±0.01)
$\langle \alpha_{lc,r,s} \rangle$/deg	69.16	69.22(±0.01)

TABLE 6: System Specifications: $T = 300$ K, $P = 1.00$ atm, $M = 720.7$ g·mol^{-1} (C_{60}), $r_A = 0.375$ nm, $N = 1{,}728$, $\langle \Delta r_{stand} \rangle \approx 0.0150$ nm, $\langle \mathbf{v} \rangle \approx 93.9$ m·s^{-1}, $r_{cont} \approx 25.6$ nm, and $\tau_{ideal} \approx 0.365$

parameter	theoretical value	simulation value
Z_{AA}/s^{-1}	4.986×10^{12}	$4.996(\pm 0.010) \times 10^{12}$
η_f	0.7071	0.7078(±0.0005)
$\langle v_{lc,f} \rangle$/m·s^{-1}	120.7	120.7(±0.1)
$\langle v_{lc,r} \rangle$/m·s^{-1}	64.68	64.65(±0.08)
λ/nm	16.27	16.24(±0.03)
p_{f-f}	0.5000	0.5023(±0.0011)
p_{r-r}	0.085 79	$0.08627(\pm 4.1 \times 10^{-4})$
p_{f-r}	0.2071	$0.2068(\pm 5 \times 10^{-4})$
p_{r-f}	0.2071	$0.2068(\pm 5 \times 10^{-4})$
$\langle v_f \rangle$/m·s^{-1}	102.2	102.3(±0.1)
$\langle v_{r,f} \rangle$/m·s^{-1}	121.3	121.4(±0.1)
$\langle v_{r,s} \rangle$/m·s^{-1}	80.98	80.99(±0.07)
$\langle \alpha_{lc,f} \rangle$/deg	51.15	51.14(±0.01)
$\langle \alpha_{lc,r,f} \rangle$/deg	39.48	39.50(±0.01)
$\langle \alpha_{lc,r,s} \rangle$/deg	69.16	69.14(±0.01)

Outside of pedagogic pursuits and classroom discussions, configuration specificity in gas-phase dynamics has several other potential applications. For one, adding configuration specificity as a higher level of analytical detail may shed some insight into certain gas-phase dynamic processes. Also, configuration

specificity may shed some light in interpreting the results of certain gas-phase experiments such as molecular beam studies.

It should be emphasized here that even though configuration specificity does add deeper understanding of gas-phase collision processes, the analysis is limited in its application due to the restrictions that the molecules are spherical and noninteracting. The general results presented in this paper become less applicable for molecules that are structured or exhibit intermolecular interactions. For one, an accurate assessment of the collision cross section becomes somewhat tenuous for structured molecules. Second, intermolecular potentials will affect the center-of-mass trajectories as well as the internal motion of structured molecules when the molecules are close enough for the force fields to interact. Of course, some of the behavioral trends for the non-configuration-specific parameters in nonideal systems can be predicted with some level of confidence. For instance, the collision frequencies will likely be larger and the mean free paths smaller for molecules that exhibit attractive interactions. On the other hand, even guessing the trends for many of the configuration-specific parameters is difficult without resorting to some level of analysis.

A follow-on paper in this series will be devoted to deriving the configuration-specific collision parameters for a binary system. It will be demonstrated that the following equation is obtained using the configuration-specific analysis:[9]

$$Z_{AB} = \sqrt{\frac{8kT}{\pi\mu}} \frac{PN\sigma_{AB}X_A(1 - X_A)}{kT} \tag{52}$$

in which μ is the reduced mass and X_A is the mole fraction for component A.

Acknowledgment. The author graciously thanks Miss Kia Tavares for her expert help in analyzing several of the integrals using *Mathematica*.

References and Notes

(1) *Physical Chemistry*; Atkins, A., de Paula, J., Eds.; W. H. Freeman and Company: New York, 2002.

(2) Serway, R. *Physics for Scientists and Engineers with Modern Physics*, 3rd ed.; Saunders College Publishing: Philadelphia, PA, 1990.

(3) *A Textbook of Physical Chemistry*; Negi, A. S., Anand, S. C., Eds.; New Age International (P) Ltd.: New Delhi, India, 2004.

(4) *Kinetic Theory of Gases*; Present, R. D., Ed.; McGraw-Hill Book Company: New York, 1958.

(5) *Introduction to Theoretical Mechanics*; Becker, R. A., Ed.; McGraw-Hill Book Company: New York, 1954.

(6) *The Mathematical Theory of Non-Uniform Gases*, 3rd ed.; Chapman, S., Cowling, T. G., Eds.; Cambridge University Press: Cambridge, U.K., 1970.

(7) *Kinetic Theory of Gases*; Kauzmann, W., Ed.; Benjamin: San Francisco, CA, 1966.

(8) *Mathematica 5.1* (Wolfram Research, 2003) has been used to perform most of the more complicated integrals in this paper.

(9) Davis, E. J. *Aerosol. Sci. Technol.* **1983**, *2*, 121.